ELSEVIER

Journal of Power Sources 68 (1997) 212–215

JOURNAL OF POWER SOURCES

Low-crystallized carbon materials for lithium-ion secondary batteries

Hayato Higuchi *, Keiichiro Uenae, Akira Kawakami

Hitachi Maxell Ltd., Battery R&D Laboratory, 1-1-88, Ushitora, Ibaraki, Osaka 567, Japan

Accepted 6 November 1996

Abstract

The charge/discharge characteristics and mechanisms of low-crystallized carbons which have larger capacity than graphite have been investigated. Low-crystallized carbons have two principal types of charge curve versus Li metal. Hard carbons prepared at 1100 °C (H11) show charge curves with a low average potential, whereas soft carbons pyrolyzed at 700 °C (S7) show those with a high average potential. These results might depend on the lithium diffusion rate in their non-crystallized sites. The 18650-type Li-ion batteries using H11 have comparable capacity versus graphite, whereas the batteries using S7 have low capacity because of their low charge/discharge efficiency.
© 1997 Published by Elsevier Science S.A.

Keywords: Carbon materials; Discharge potential, Lithium-ion batteries, Lithium diffusion coefficient

1. Introduction

Lithium-ion secondary batteries are currently of interest as high-energy power sources for electronics. Further increase in energy density of these batteries requires increase in specific capacities of the electrode materials. In recent years, carbon-based materials have been extensively studied as the anodes of these batteries. There have been many reports of low-crystallized carbons with capacities greater than that of graphite (C_6Li at 372 mAh/g) [1–8]. For example, carbons made by pyrolyzing pitch at 700 °C [1,2], polyparaphenylene (PPP) [3] and polyacenic semiconductor (PAS) [4] were shown to have capacities of up to 700 mAh/g. Pyrolyzed polyfurfuryl alcohol with capacities near 450 mAh/g have been prepared by Omaru et al. [5]. Low-crystallized carbons have been observed to have two types of charge curve versus lithium metal depending on the raw materials used (precursor) and/or the heat-treatment temperature: the first type shows charge curves similar to graphite with a low average potential versus Li/Li^+, and the other has charge curves with a high average potential. Each charge potential would be affected by the electrochemical potential of lithium doped in non-crystallized sites in addition to the interlayer. In order to discuss the relationship between the lithium doping/undoping mechanisms for low-crystallized carbons and the charge potential, the lithium diffusion coefficients in each carbon sample was measured.

The characteristics of lithium-ion batteries with anodes using these low-crystallized carbons have been studied.

2. Experimental

2.1. Measurements of unit cell performances and lithium diffusion coefficients

The carbon materials are prepared by the pyrolytic treatment of resin at 1100 °C (shows H11 as follows), and of mesophase pitch coal tar at 700 °C (S7) and 3000 °C (S30). The carbon powders were mixed with a solution of 10 wt.% polyvinylidene fluoride (PVDF) dissolved in *n*-methyl-2-pyrrolidine (NMP). The slurry was spread as a thin layer on a copper foil using the doctor blade method. After coating, the electrodes were pressed at 40 kg/cm^2 and at 120 °C. The electrodes were set in polypropylene cells in a parallel plate configuration using lithium foil counter electrode and a lithium reference electrode. The electrolytes were 1 M $LiPF_6$ dissolved in a 50/50 by volume mixture of ethylene carbonate/methylethyl carbonate (EC/MEC). The cells were discharged by the constant current–constant voltage method (CC–CV). A constant current of 0.5 mA/cm^2 is applied until 0 V versus Li/Li^+ is reached. Then the constant voltage (0 V) is maintained until 10 μA/cm^2 is reached. The cell is then charged to 1.5 V at 0.5 mA/cm^2. The open-circuit voltage (OCV) was measured after 1 h at open-circuit conditions after polarization at 0.1 mA/cm^2.

* Corresponding author.

0378-7753/97/$17.00 © 1997 Published by Elsevier Science S.A. All rights reserved
PII S0378-7753(96)02587-6

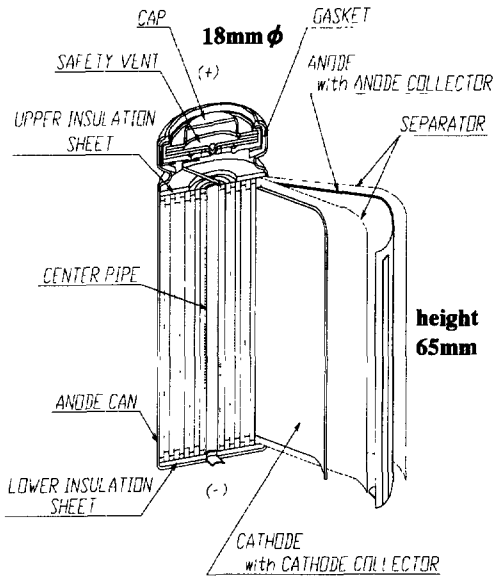

Fig 1 Structure of the 18650-type cylindrical Li-ion battery.

The lithium diffusion coefficients (D_{Li}) were calculated from the Warburg impedance by potentiostatic a.c. impedance method [9,10]. The impedance measurements carried out under open-circuit conditions in the frequency range from 10^{4} to 10^{-2} Hz. The perturbation amplitude was ± 5 mV.

2.2. 18650-type cylindrical cell

Fig. 1 shows the 18650-type cylindrical battery (diameter: 18 mm and height: 65 mm) consisting of a spirally rolled cathode, $LiCoO_2$, and an anode inserted in the polyethylene separator. The electrolytes were same as described in Section 2.1. Cell cycling is done by the CC–CV method, in which the constant current is at 1C rate (1300 mA) and the constant voltage is maintained at 4.2 V. The cut-off voltage of discharge is 2.75 V (for H11 and S30) or 2.3 V (for S7), respectively.

3. Results and discussion

3.1. Charge/discharge characteristics of low-crystallized carbons

Fig. 2 shows the charge/discharge OCV curves of the first cycle of the H11, S7 and S30 electrodes. The charge capacities of H11, S7 and S30 versus Li/Li^+ below 1 V indicated 400, 600 and 330 mAh/g, and the charge/discharge efficiency of the first cycle showed 80, 59 and 92%, respectively. For H11 most of the capacity during charge is at a low potential similar to that during discharge. This behavior is similar to that of graphite (S30). For S7 most of the capacity during charge is at a higher potential than that during discharge. However, most of the capacity for both H11 and S7 during discharge is at a lower potential (near 0 V) than that of S30. Fig. 3 shows the cycle characteristics of H11 and S7 for

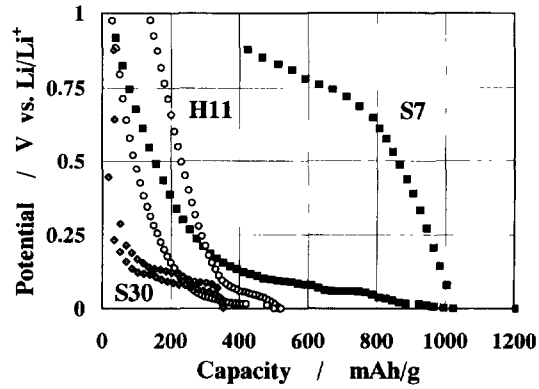

Fig. 2. Open-circuit voltage curves at the first cycle for the H11, S7 and S30 electrodes.

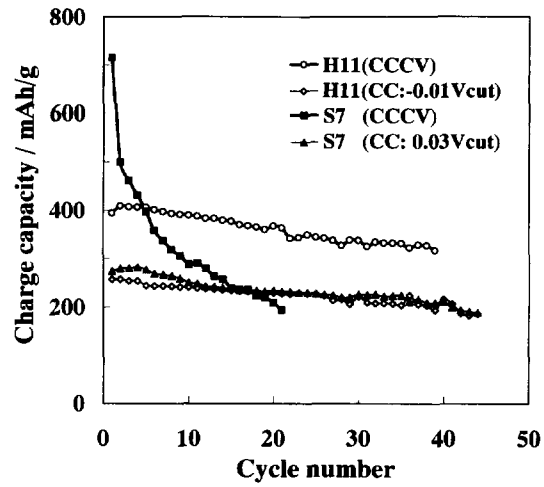

Fig. 3. Charge/discharge cycle characteristics for the H11 and S7 electrodes for different depths-of-discharge.

different depths-of-discharge. As the discharge capacity increased, the cycle characteristics deteriorated, especially for S7.

Fig. 4 shows the relationship between D_{Li} and the charge/discharge capacities for H11, S7 and S30. As D_{Li} in graphite (S30) always exceeded $10^{-6.8}$ cm^2/s, D_{Li} for H11 and S7 decreased between the beginning and the end of discharging below 10^{-7} cm^2/s (smaller than S30). Low D_{Li} (decreasing with increasing discharge capacity) in H11 and S7 (low-crystallized carbons) limited by a lithium diffusion rate in non-crystallized sites. This is in contrast with S30 which has a higher D_{Li} limited by an intercalation process. The capacity decrease during cycling of low-crystallized carbons may be a result of damaged non-crystallized sites.

Further, during charging D_{Li} for H11 increased reversibly versus discharging, whereas D_{Li} for S7 decreased with irreversible charge/discharge process. The decrease in D_{Li} could cause an increase in diffusion over potential. Therefore, the diffusion over potential of S7 would increase with charging, leading to charge curves with a high potential, as observed.

Table 1 summarizes true density and X-ray diffraction (XRD) data as well as the hydrogen:carbon atomic ratio for the samples. The average layer spacing (d_{002}) of H11 is

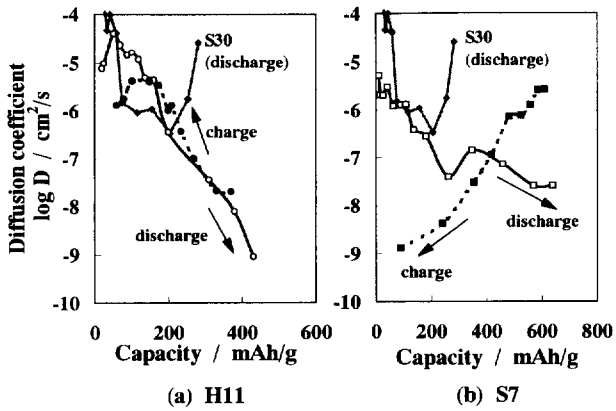

Fig. 4 Lithium diffusion coefficient (D_{Li}) vs charge/discharge capacity for H11, S7, S30

Table 1
Summary of the carbon samples

Sample	Origin	HTT (°C)	True density (g/cm³)	d_{002} (Å)	L_c (Å)	H/C ratio
H11	Resin	1100	1.59	3.80	13	0.02
S7	Mesophase	700	1.53	3.61	16	0.26
S30	Pitch coal tar	3000	2.21	3.36	1000	<0

greater than that of S7. However, crystallized size along the c-axis (L_c) of both H11 and S7 are almost similar. The structure of H11 indicates a minor number of stacking layers, therefore lower crystallized than S7 in spite of a higher heat-treatment temperature. The hydrogen:carbon ratio of H11 is nearly 0 similar as that of S30, whereas that of S7 is greater. It might therefore be presumed that each charge potential is influenced by the charge mechanisms involving the non-crystallized sites, as illustrated in Fig. 5. For charge mechanism of S7, lithium doped into non-crystallized sites may be inactivated by the C(layer)–Li interaction and/or interference lithium undoping of the hydrogen atom. The charge for S7 therefore would proceed by de-intercalation of lithium prior to undoping from non-crystallized sites.

3.2. 18650-type battery performances

Fig. 6 shows discharge characteristics of 18650-type batteries using the H11, S7 and S30 anodes. The battery using H11 has a discharge capacity of approximately 1300 mAh from 4.1 to 2.75 V similar to the battery using S30. The battery using S7 shows a lower capacity and a lower voltage than S30 because of the remarkably low charge/discharge efficiency on the first cycle and low potential versus Li/Li$^+$ during lithium de-insertion. Our batteries which use low-crystallized carbons have a low capacity, even though the low-crystallized carbons have a higher capacity than graphite. This is due to the electrode densities of low-crystallized carbons. The electrode density of H11 and S7 is lower (1.1 g/cm³) than that of S30 (1.6 g/cm³), leading to a lower volumetric energy density for electrodes made from H11 and S7 than for electrodes made from S30.

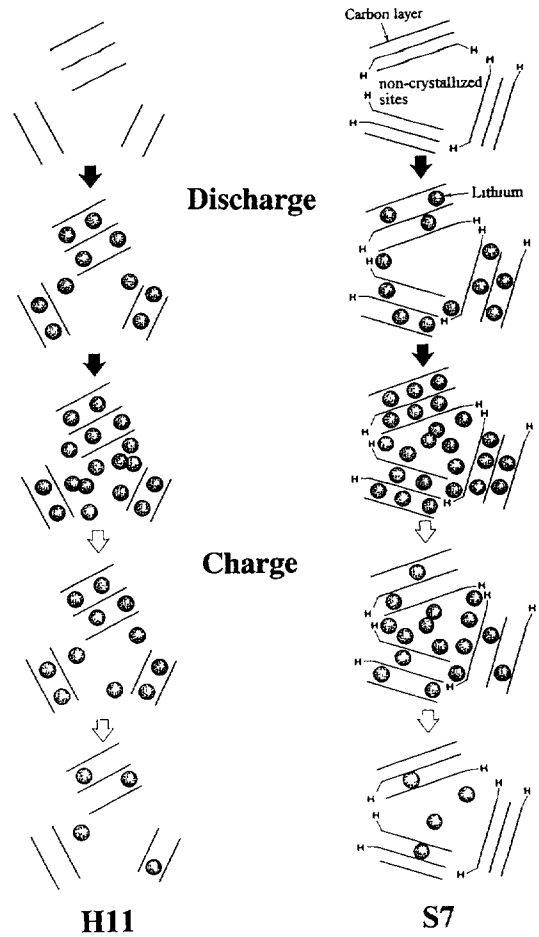

Fig. 5. Schematic illustration for the charge/discharge mechanisms of H11 and S7.

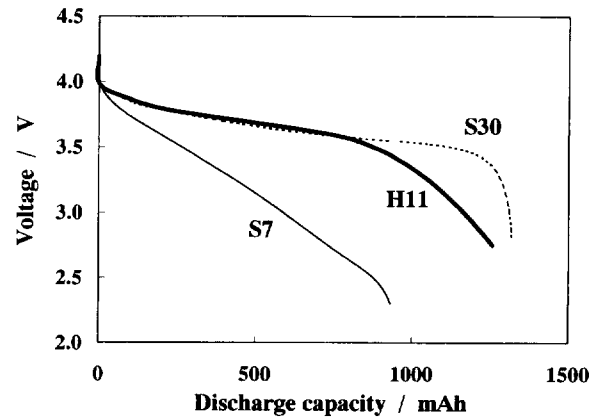

Fig. 6. Discharge characteristics of the 18650-type Li-ion battery using the H11, S7 and S30 anodes; 1C (1300 mA), 4.2 V CC–CV charge; 1C, 2.75 V cut discharge.

Fig. 7 shows charge/discharge cycle characteristics of 18650-type batteries using H11 anode in the case of the variation of charge capacities. Cycling the 100% depth-of-discharge of the capacity of H11 (400 mAh/g) of this battery at initial cycle, the capacity after 200 cycles was below 50% of initial capacity, whereas under the 67.5% depth (270 mAh/g), the capacity after 500 cycles remained 100% of

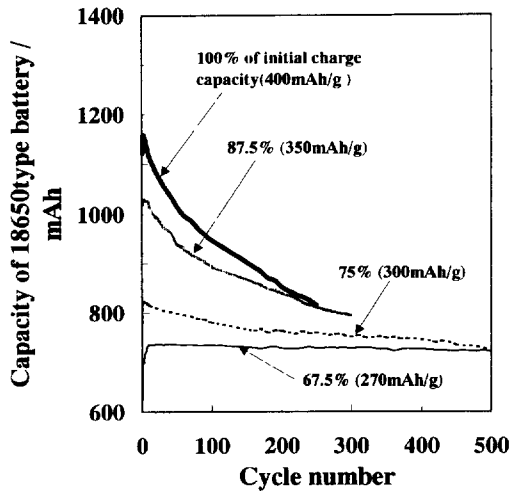

Fig. 7 Charge/discharge cycle characteristics of the 18650-type Li-ion battery using the H11 anode

initial one, and the charge/discharge efficiency was almost 100%. Therefore, the cycle characteristics are affected by the charge depths similar to the unit cells (see Fig. 3). This causes to be considered are: (i) damaged lithium doping sites, especially non-crystallized sites; (ii) decrease of the electric conductivity of the electrode versus increase of the cell resistance with cycle, and (iii) influence of lithium metal deposition on the anode surface.

4. Conclusions

The low-crystallized carbons have two types of the discharge curves: (i) charge curves with a low potential versus Li/Li^+, e.g. the pyrolytic treatment of the resin at 1100 °C (H11) which has a charge capacity of 400 mAh/g, and (ii) charge curves with a high potential, e.g. that of coal tar pitch at 700 °C (S7) which has a charge capacity of 600 mAh/g. This high potential during charge corresponds with the removal of lithium from non-crystallized sites after most interlayer lithium sites have been emptied.

The 18650-type batteries using the H11 anode have capacities comparable with 18650-type batteries using the S30 anode, although the capacity of the H11 cells decreased with cycling at 100% of the H11 initial capacity. On the other hand, the batteries using S7 have a lower capacity because S7 shows a low charge/discharge efficiency and a high potential versus Li/Li^+ during lithium removal.

References

[1] A. Mabuchi, K. Tokumitsu, H. Fujimoto and Kasue, *J. Electrochem Soc., 142* (1995) 1041.
[2] A Satoh, N. Takami, T Ohsaki and M. Kanda, *Ext. Abstr , Fall Meet. The Electrochemical Society, 1994*, Abstr No. 91.
[3] K. Sato, M. Noguchi, A. Demachi, N. Oki and M. Endo, *Science, 264* (1994) 556.
[4] S Yata, H. Kinoshita, M. Komori, N. Ando, T Kashiwamura, T. Harada, K. Tanaka and T. Yamabe, *Synth. Met., 62* (1994) 153.
[5] A Omaru, H. Azuma, M. Aoki, A. Kita and Y. Nishi, *Ext. Abstr., Meet The Electrochemical Society, 1992*, Abstr. No. 25
[6] T Zheng, Y. Liu, E.W. Fuller, S. Tseng, U von Sacken and J.R. Dahn, *J. Electrochem. Soc., 142* (1995) 2581.
[7] R. Yazami and M. Deschamps, *36th Battery Symp. Japan, 1995*, p 3I07L.
[8] Y. Takahashi, J. Oishi, Y. Miki, M. Yoshimura, K. Shibahara and H. Sakamoto, *35th Battery Symp. Japan, 1995*, p. 2B05.
[9] N. Takami, A Satoh, M. Hara and T Ohsaki, *J. Electrochem. Soc., 142* (1995) 371.
[10] T.B. Hunter, P.S. Tyler, W.H. Smyrl and H S. White, *J. Electrochem. Soc., 132* (1995) 2198.